Csf2 and *Ptgs2* Epigenetic Dysregulation in Diabetes-prone Bicongenic B6.NODC11bxC1tb Mice

Erin Garrigan[1,*,†], Nicole S. Belkin[1,*,†], Federica Seydel[1,*,†], Zhao Han[1], Jamal Carter[1,†], Marcia McDuffie[2], Laurence Morel[1], Ammon B. Peck[1], Michael J. Clare-Salzler[1], Mark Atkinson[1], Clive Wasserfall[1], Abdoreza Davoodi-Semiromi[1,†], Jing-da Shi[3,†], Carrie Haskell-Luevano[4,†], Li-Jun Yang[1], John J. Alexander[1,†], Autumn Cdebaca[5,†], Teresa Piliant[5], Corin Riggs[5,6], Matthew Amick[1,6] and Sally A. Litherland[1,6,7]

[1]Department of Pathology, Immunology, and Laboratory Medicine, College of Medicine, University of Florida, Gainesville, FL, USA. [2]School of Medicine, University of Virginia, Charlottesville, VA, USA. [3]Department of Biochemistry and Molecular Biology, College of Medicine, University of Florida, Gainesville, FL, USA. [4]Department of Pharmacodynamics, College of Pharmacy, University of Florida, Gainesville, FL, USA. [5]Bionetics Corporation, Kennedy Space Center, FL, USA. [6]Sanford-Burnham Medical Research Institute, Diabetes and Obesity Center, Lake Nona-Orlando, FL, USA. [7]Florida Hospital Cancer Institute, Orlando, FL, USA. *These authors contributed equally to the work of this study. †Current addresses: E. Garrigan: Department of Pediatrics, College of Medicine, University of Florida, Gainesville, FL, USA. N. Belkin: Department of Orthopaedic Surgery, University of Pennsylvania, PA, USA. F. Seydel: Department of Biochemistry and Molecular Medicine, University of California–Davis, CA, USA. J. Carter: Department of Pathology, Johns Hopkins University, Baltimore, MD, USA. J. Shi: ICBR, University of Florida, Gainesville, FL, USA. A. Davoodi-Semiromi: Miller School of Medicine, Miami, FL, USA. C. Haskell-Luevano: Department of Medicinal Chemistry, University of Minnesota, Minneapolis, MN, USA. J.J. Alexander: Department of Human Genetics, Atlanta, GA USA. R. Bober: Enterprise Advisory Systems/NASA, Kennedy Space Center, FL USA. A. Cdebaca: Enterprise Advisory Services/NASA, Kennedy Space Center, FL, USA.

ABSTRACT: In Type 1 diabetic (T1D) human monocytes, STAT5 aberrantly binds to epigenetic regulatory sites of two proinflammatory genes, *CSF2* (encoding granulocyte–macrophage colony-stimulating factor) and *PTGS2* (encoding prostaglandin synthase 2/cyclooxygenase 2). Bicongenic B6.NOD C11bxC1tb mice re-create this phenotype of T1D monocytes with only two nonobese diabetic (NOD) *Idd* subloci (130.8 Mb–149.7 Mb, of *Idd5* on *Chr 1* and 32.08–53.85 Mb of *Idd4.3* on *Chr11*) on C57BL/6 genetic background. These two *Idd* loci interact through STAT5 binding at upstream regulatory regions affecting *Csf2* (*Chr 11*) and *Ptgs2* (*Chr 1*) expression. B6.NODC11bxC1tb mice exhibited hyperglycemia and immune destruction of pancreatic islets between 8 and 30 weeks of age, with 12%–22% penetrance. Thus, B6.NODC11bxC1tb mice embody NOD epigenetic dysregulation of gene expression in myeloid cells, and this defect appears to be sufficient to impart genetic susceptibility to diabetes in an otherwise genetically nonautoimmune mouse.

KEYWORDS: epigenetic gene regulation, inflammation, autoimmune, diabetes, cytokine, congenic mice

CITATION: Garrigan et al. *Csf2* and *Ptgs2* Epigenetic Dysregulation in Diabetes-prone Bicongenic B6.NODC11bxC1tb Mice. *Genetics & Epigenetics* 2015:7 5–17 doi:10.4137/GEG.S29696.

TYPE: Original Research

RECEIVED: May 13, 2015. **RESUBMITTED:** June 21, 2015. **ACCEPTED FOR PUBLICATION:** June 23, 2015.

ACADEMIC EDITOR: Christian Bronner, Editor in Chief

PEER REVIEW: Four peer reviewers contributed to the peer review report. Reviewers' reports totaled 537 words, excluding any confidential comments to the academic editor.

FUNDING: This work was supported by grants to SAL from the NIH/NIDDK (DK002947 & DK08082) and the JDRF (33-2008-407) and to MAtkinson/MJCS from the NIH/NIAID (PO1 AI42288). The authors confirm that the funders had no influence over the study design, content of the article, or selection of this journal.

COMPETING INTERESTS: Authors disclose no potential conflicts of interest.

CORRESPONDENCE: sally.litherland@flhosp.org

Paper subject to independent expert blind peer review. All editorial decisions made by independent academic editor. Upon submission manuscript was subject to anti-plagiarism scanning. Prior to publication all authors have given signed confirmation of agreement to article publication and compliance with all applicable ethical and legal requirements, including the accuracy of author and contributor information, disclosure of competing interests and funding sources, compliance with ethical requirements relating to human and animal study participants, and compliance with any copyright requirements of third parties. This journal is a member of the Committee on Publication Ethics (COPE).

Published by Libertas Academica. Learn more about this journal.

Introduction

Granulocyte–macrophage colony-stimulating factor (GM-CSF) expression is normally tightly regulated in the sequence of cytokines in myeloid cell hematopoiesis, coming after interleukin (IL)-3 simulation of peri-potent bone marrow stem cells, but before macrophage colony–stimulating factor (M-CSF)'s influences in differentiation.[1] GM-CSF allows premyeloid bone marrow cells to progress toward specific pre-myeloid cell subtypes, differentiating into granulocytes, monocytes, macrophages, and dendritic cells.[1–4] Cell responsiveness to GM-CSF must be suppressed for the subsequent lineage-specific cytokines (G-CSF, M-CSF) to complete the maturation process.[1] If not, cells will progress to intermediate proinflammatory phenotypes or suffer elimination in the process.[1,4,5]

After M-CSF stimulation in differentiation, mature monocytes and macrophages can again respond to GM-CSF, though now as an activation, not a differentiation, stimulant.[1,2] In inflammation, mature myeloid cells produce GM-CSF in response to toll-like receptor (TLR)-induced activation and inflammatory IL-6 and IL-1β cytokine signaling.[6,7] Within the first 4–6 hours of an immune inflammatory response, GM-CSF supports the activation of prostaglandin synthase 2/cyclooxygenase 2 (PGS2/COX2), the dual-function enzyme involved in early response proinflammatory prostanoid

production.[8,9] GM-CSF also induces IL-10 production and responsiveness in the cells approximately 10 hours after the initial insult, allowing for normal resolution of inflammation and a return to homeostasis.[1,8]

Such tight temporal regulation of GM-CSF expression relies heavily on cytokine-induced epigenetic control of chromatin upstream of its coding region, through histone acetylation/deacetylation modifications. Several sequence-specific sites in the *Csf2* promoter have been described as association sites for the histone deacetylase, silencing mediator of retonoid (SMRT)/nuclear receptor co-repressor (NCoR), in response to IL-6, IL-1β, and IL-2 activation of this gene in myeloid cells and T cells.[10,11] Anti-inflammatory drugs such as indomethacin and glucocorticords exert their anti-inflammatory effects through modulation of histone acetylation/deacetylation enzymes working at specific sites within the *Csf2* promoter.[6,7]

Autoimmune myeloid cells overproduce GM-CSF, allowing for persistent activation of the signal transduction/transcriptional regulatory proteins, STAT5A and STAT5B (STAT5). STAT5 proteins can act as secondary signal molecules for cytokine signaling and adaptor proteins epigenetic histone modification enzymes including SMRT/NCoR to promote histone deacetylation and CREB binding protein (CBP)/protein 300 (P300) acetylase for histone acetylation.[10–12] In nonobese diabetic (NOD) mouse and Type 1 diabetic (T1D) human monocytes and macrophages, activated STAT5 proteins exhibit aberrant DNA binding and subcellular localization.[13] Human T1D monocytes have aberrant STAT5 binding at an enhancer sequence upstream of the *PTGS2* gene concurrent with CBP/P300 histone acetylase and RNA polymerase II binding and acetylation of histone H3 at the same location.[14] Congenic mouse analysis revealed that similar STAT5 and GM-CSF traits are linked to NOD polymorphisms in the *Idd4.3* diabetes susceptibility region of NOD chromosome 11.[13,15,16] The *Idd4.3* region contains the gene for GM-CSF, *Csf2*, along with several other cytokines that use STAT5 in their signaling.[16–18]

In this study, we use congenic mouse strains derived from NOD and two nonautoimmune mouse strains (C57BL/6 and C57L) to investigate whether GM-CSF activation of STAT5 binding at epigenetic regulatory sites within the *Csf2* gene promoter alters its regulation of its own expression as well as that of *Ptgs2*, the gene for PGS2/COX2, found near the *Idd5* on NOD Chr 1.[18] Previous findings indicated that GM-CSF regulates STAT5 binding to chromatin in the NOD noncoding sequence upstream of *Csf2*, in regions previously reported as epigenetic modification sites within the *Csf2* promoter.[6,7,19] This study's findings suggest that endogenous NOD level expression of *Csf2* or the addition of exogenous GM-CSF promoted STAT5 binding at the enhancer of *Ptgs2*, affecting PGS2/COX2 expression and activity in NOD and NOD congenic mouse myeloid cells. Congenic breeding of the *Csf2* and *Ptgs2* containing NOD loci onto C57BL/6 mice not only allowed interaction of these two *Idd* loci (*Idd4.3* on Chr 11 and *Idd5* on Chr 1) via STAT5 binding and epigenetic modulation but was also sufficient to support the development of diabetic hyperglycemia and immune-mediated islet cell destruction at a low but consistent penetrance in B6.NODC11bxC1tb bicongenic mice.

Materials and Methods

Mouse strains. Ethics statement: All procedures were conducted according to Institutional Animal Care and Use Committee (IACUC) approved protocols at the University of Florida (UF), Kennedy Space Center Space Life Sciences Laboratory, and Sanford-Burnham Medical Research Institute (SBMRI) at Lake Nona, Florida. This study was carried out in strict accordance with the recommendations in the Guide for the Care and Use of Laboratory Animals of the National Institutes of Health. All efforts were made to minimize suffering and provide humane treatment for the animals used in this study.

Three- to 20-week-old NOD, C57BL/6, and C57L female and male mice (The Jackson Laboratory, Bar Harbor, ME, USA) were used in these studies. At least two mice of each strain were used for tissues per analysis, and each analysis was run at minimum in triplicate. These strains were maintained as breeding stock in the University of Florida College of Medicine Pathology Department Specific Pathogen Free (SPF) colony, in microisolator cages with food and water ad libitum. Figure 1 gives a schematic representation of the regions on chromosomes contributed by NOD, C57BL/6, and C57L parental strains in the NOD.LC11[17] and B6.NODC11[16,18] congenic strains used in this study. Subcongenic strains of the B6.NODC11 and NOD.LC11 mice (labeled with letters after C11 in their names, Fig. 1) were bred by backcross to C57BL/6 then intercross as in speed congenic protocols previously described.[18,20]

NOD background subcongenic strain NOD.LC11 (NOD.L-(D11Mit314-D11Mit42)/McdfJ; now available from Jackson Laboratory, stock #008053) and its subcongenic recombinant derivatives NOD.LC11b (NOD.L-(D11Mit314-*Csf2*)/McdfJ; Jackson Lab stock #008055) and NOD.LC11e (NOD.L-(*Csf2*-D11Mit339)/McdfJ; Jackson Lab stock #008056) were developed at the University of Virginia.[17] NOD.LC11e mice carry a C57L interval covering the *Csf2* gene for GM-CSF and *Idd4* interval, but excluding the promoter region (Fig. 2). NOD.LC11b contains a C57L region, which includes the *Idd4.3* region down through the *Csf2* gene but excludes all the regions telomeric and downstream of the *Csf2* gene.

The B6.NODC11b and B6.NODC1tb subcongenic mouse strains were derived for this study from backcrossing the B6.NODC11 and B6.NODC1 mice in the University of Florida Department of Pathology SPF Mouse colony, which were originally derived by Yui and Wakeland,[1] with C57BL/6J mice from Jackson Laboratory for three to five generations then intercrossing the offspring for three generations to homozygosity. Each subcongenic line was intercrossed for at least three more generations to establish the strains depicted in Figure 1. These subcongenic mice do not develop diabetes but have periductal insulitis (data not shown).

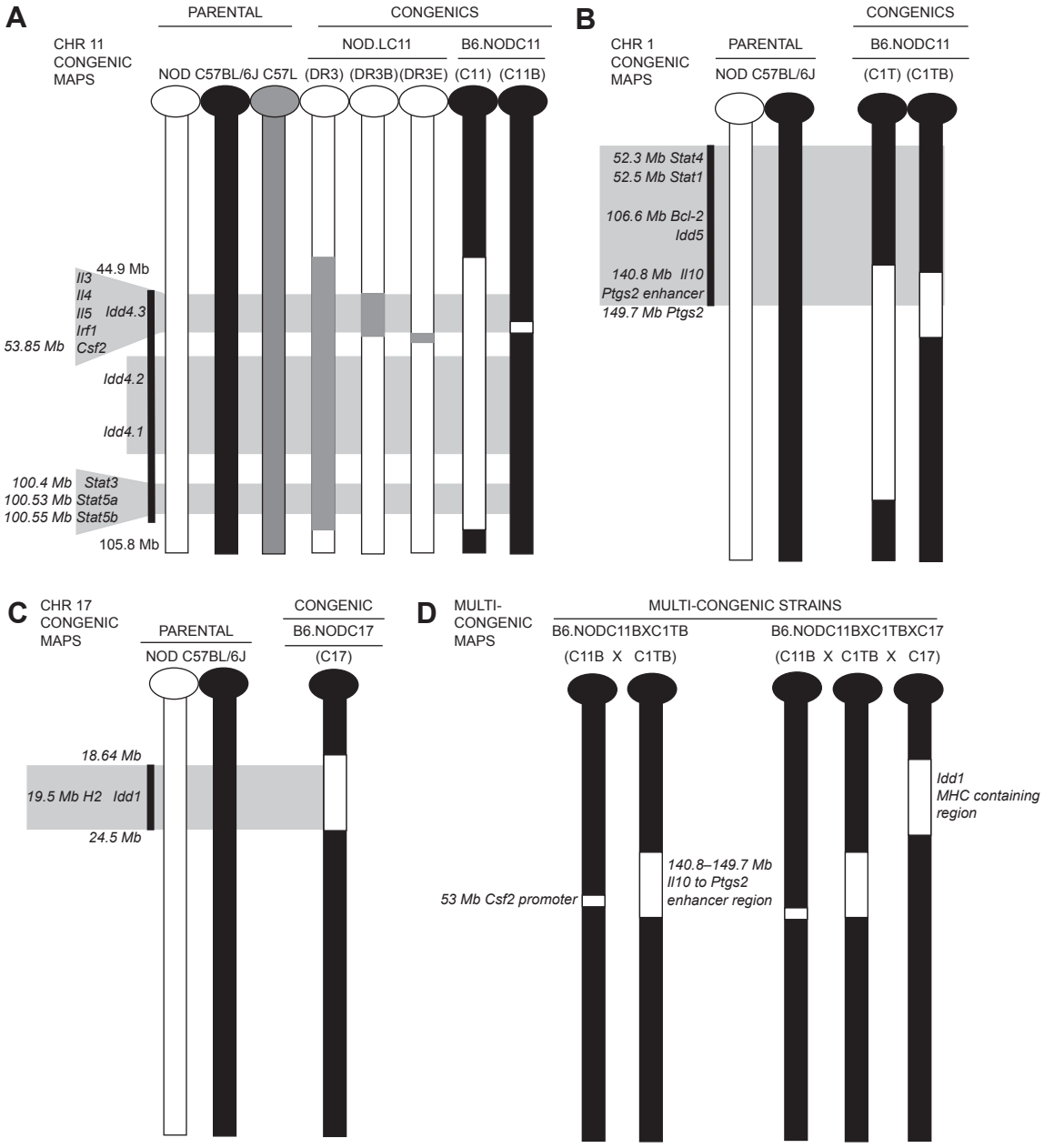

E PHENOTYPE SUMMARY

PHENOTYPE/STRAIN	DIABETES INCIDENCE	INSULITIS	%STAT5 PTYR/ CD11b+ CELLS	GM-CSF (pg/10^6 CELLS)	PGE2 (pg/10^6 CELLS)	PGS2/COX2
NOD	65–80%	INVASIVE	40	66	39	POSITIVE; IL10 RESISTANT & GM-CSF INDUCIBLE
C57BL/6J	0	–	15	16	14	NEGATIVE; IL10 SENSITIVE
C57L	0	–	<1	16	ND	ND
NOD.LC11	<2%	PERI ISLET	7	6	4	POSITIVE; IL10 SENSITIVE
NOD.LC11B	<27%	PERI ISLET	3	18	15	NEGATIVE; GM-CSF INDUCIBLE
NOD.LC11E	>65%	INVASIVE	8	91	6	POSITIVE; GM-CSF ENHANCED
B6.NODC11	0	PERI DUCTAL	20	82	52	NEGATIVE; IL10 SENSITIVE
B6.NODC11B	0	PERI DUCTAL	7	50	4	NEGATIVE; IL10 SENSITIVE
B6.NODC1T	0	PERI DUCTAL	0	13	42	POSITIVE; IL10 SENSITIVE
B6.NODC1TB	0	PERI DUCTAL	0	0	0	POSITIVE; GM-CSF ENHANCED
B6.NODC17	0	PERI ISLET	0	0	0	NEGATIVE
B6.NODC11BXC1TB	12–22%	INVASIVE	30	8	244	POSITIVE; GM-CSF ENHANCED
B6.NODC11BXC1TBXC17	23–42%	INVASIVE	45	2	68	POSITIVE; GM-CSF ENHANCED

Figure 1. Summary of congenic mouse chromosomal maps for chromosomes 11, 1, and 17. Color indicates the genetic origin of the sequences on Chr 11 (**A**), Chr 1 (**B**), and Chr 17 (**C**) and in the multi-congenic strains (**D**): black = C57BL/6, grey = C57L, and white = NOD. The location of *Idd* and other regions/genes of interest are listed on the left side of the maps and highlighted across the maps by the shaded horizontal areas. Strain names and shorthand identifiers (in parentheses) are listed at the top of the maps. (**E**) Summary of the current phenotypic findings for each strain including data from the current study as well as our previously published work[13,15,16,19] and that of others.[17,18] Histological phenotype scoring by three blinded reviewers are indicated as Peri = infiltration around pancreatic inlets; invasive = destructive islet infiltration; '–' = no infiltrate seen.

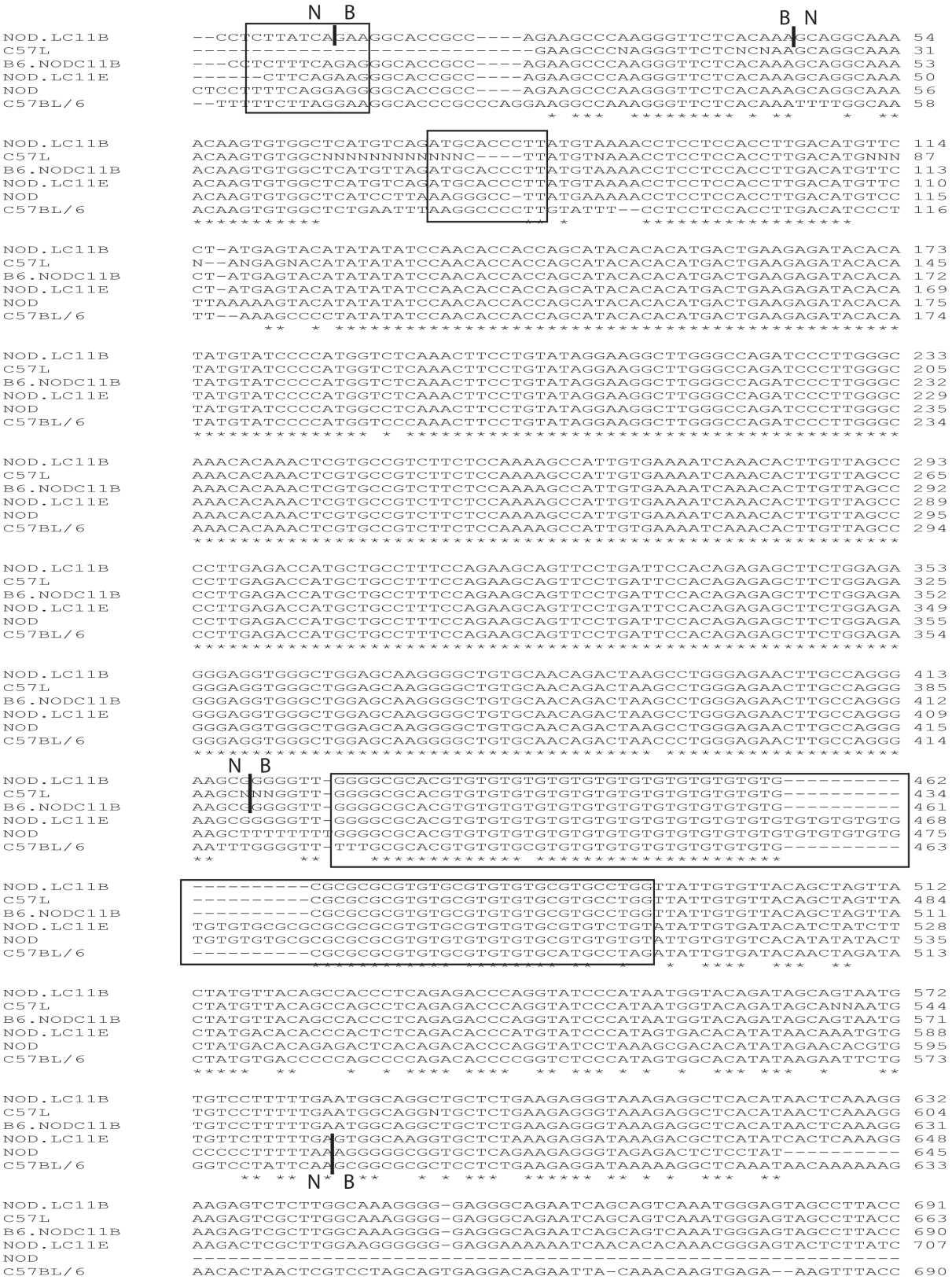

Figure 2. Sequence analysis of *Csf2* promoter region and definition of the STAT5 binding site polymorphisms involved in NOD myeloid cell phenotypes and chromosome 11 diabetes susceptibility. Genomic DNA from each congenic and parental strain was prepared from liver and amplified in PCR using primers designed to amplify the −969 bp to −3 bp sequence upstream of the *Csf2* gene.[6,7] Boxed sequences indicate potential STAT protein consensus binding sequences (CTTNNN(N)GAA) and microsatellite polymorphism seen in NOD compared to the GT repeat seen in control strains C57BL/6 and C57L. Dashed areas indicate gaps in sequence of some strains (ie, base pairs not found in some strains) indicated by CLUSTAL alignment. Vertical lines indicate sites of transition between NOD and control strain DNA sequences in congenic strains. N = NOD genetic sequence; B = control strain (C57BL/6 for B6.NODC11b strain; C57L for NOD.LC11E and NOD.LC11B strains). Asterisks (*) indicate sequence homology across all strains.

The B6.NOD congenic mice, along with NOD and C57BL/6 mice purchased from Jackson Laboratories, were originally bred and housed in the University of Florida SPF colony. The strains used in these studies were maintained at the University of Florida, Kennedy Space Center, and later at the new SBMRI at Lake Nona SPF vivarium facilities.

Diabetes incidence in the NOD.LC11 and B6.NODC11 and B6.NODC1 strains was measured by blood and urine glycemia and confirmed by pathological review of immune infiltration and beta cell destruction in pancreatic tissues as previously described.[16–18] Genotype analysis on tail or ear biopsy tissue was routinely performed at weaning of subcongenic litters to confirm maintenance of NOD genetic intervals and C57BL/6 background genetics at all other *Idd* loci were done using microsatellite polymorphism polymerase chain reaction (PCR) analysis as described by Yui et al[18] and McDuffie.[17]

Development of multicongenic strains B6.NODC11 bxC1tb and B6.NODC11bxC1tbxC17. Subcongenic line mice, B6.NODC11b, and B6.NODC1tb mice were crossbred for two to three generations and the offspring that were homozygotic NOD at each allele were bred to their siblings for five more generations to establish the bicongenic line, B6.NODC11bxC1tb (sperm available through Jackson Laboratory). The line was then bred for at least five more generations to stabilize the strain and has been maintained by homozygotic offspring breeding for over 15 generations, with breeder changes at least every 6 months. B6.NODC11bxC1tb mice were genotyped at all *Idd* intervals on chromosomes 1–19 originally described for their single congenic ancestors[18] and found to be only carrying NOD genotype alleles at the intervals depicted in maps of Figure 1 and sequence in Figure 2, including two possible STAT CCTNNN(N)GAA consensus binding sites (one found in NOD, the other in C57BL/6). This strain bred well and was exceptionally good at nurturing of litters, including being excellent at fostering other strain pups. There was a low incidence of stillbirth (3 litters over 15 generations), congenial cranial bone deformity in later generation (3 mice over 15 generations), sterile hermaphrodites (2/15 generations), and even lower incidence of cataract development (1 mouse/15th generation). Invasive, destructive insulitis scored by three blinded pathologist readers for this strain was 3/38 females (8%) and 5/30 males (16%), starting at 9 weeks of age through to 30 weeks of age. Hyperglycemia was seen in 2/18 females (11%) and 7/23 males (30%).

B6.NODC17 mice maintained for over 20 generations in the University of Florida Department of Pathology SPF Mouse colony, which were originally derived by Yui and Wakeland,[18] were bred to B6.C11bxC1tb mice for three to five generations and Chr11/Chr1/Chr17 multi-congenic line mice were established out of heterozygotic breeding of sibling pairs for two to three generations and then maintained by breeding homozygotic offspring in sibling mating for an additional five generations. The line has been maintained for over 12 generations to create the triple congenic strain, B6.NODC11bxC1tbxC17. This strain bred poorly and was very poor at nurturing of litters, especially prone to male parent infanticide and female failure to lactate. There was a high incidence of stillbirth and miscarriages (18 litters over 12 generations). Invasive, destructive insulitis scored by three blinded pathologist readers for this strain was 4/18 females (22%) and 6/24 males (25%), starting at 9 weeks of age through to 30 weeks of age. Hyperglycemia was seen in 5/21 females (24%) and 18/34 males (53%).

Tissue collection, cell culture, and sample preparation. Subcongenic and bicongenic strain mice were analyzed at weaning (3–4 weeks) through to 30 weeks of age when retired from breeding. Blood monocytes were collected from 3- to 4-week-old pups at the time of tail or ear tissue biopsy, from tail or cheek vein collection on live adult mice or from cardiac puncture postmortem after euthanasia. Mice were euthanized by overanesthetizing and cervical dislocation. After blood collection, the peritoneal cavity was filled with ice-cold RPMI medium supplemented with 10% fetal calf serum and 1% antibiotic/antimycotic mix (Cellgro-Mediatech, Herndon, VA, USA) using a 20-gauge needle and syringe. The lavage fluid and cells were withdrawn and washed with cold media by centrifugation. Liver tissue was collected after lavage for use in genomic DNA preparation, along with salivary gland and pancreatic tissues for histology. After lavage, long bones from the hind limbs were then collected and bone marrow flushed out of the bones using a 30-gauge needle and syringe filled with ice-cold RPMI medium supplemented with 10% fetal calf serum and 1% antibiotic/antimycotic mix (Cellgro-Mediatech).

The bone marrow and lavage cells were washed with cold media and then the red blood cells in samples were lysed by incubation in sterile cold 0.84% NH_4Cl buffer. The remaining cells were then plated on tissue culture dishes and fed with fresh sterile medium for culture at 37°C/5% CO_2. After 1 hour of incubation, lavage cell cultures were washed clear of nonadherent cells and the remaining adherent macrophages were refed with medium. The bone marrow and macrophage cultures were maintained in medium alone or with 1000 U/mL of GM-CSF (Biosource/Invitrogen, Carlsbad, CA, USA) or with 2 mg/mL anti-GM-CSF–blocking antibodies (Endogen/Pierce, Rockville, IL, USA) for 15 minutes to 24 hours at 37°C/5% CO_2. After the media harvest, the cells were fixed in situ with 1% (v/v C_f) formaldehyde (methanol-free, Sigma-Aldrich, St Louis, MO, USA) added in the remaining media for 10 minutes at 37°C, then washed with 1 × phosphate-buffered saline (PBS) and sonicated in sodium dodecyl sulfate (SDS) lysis buffer (Upstate/Millipore, Chicago, IL, USA) + protease inhibitors (Roche, Indianapolis, IN, USA) for later analysis in chromatin immunoprecipitation (ChIP).[19,21]

Pancreatic histology was confirmed in tissues collected at necropsy and processed through hematoxylin and eosin staining by either the University of Florida Pathology Core or the SBMRI Histology Core. Slides were examined by three blinded readers at the University of Florida and compared with the coded identification by the authors kept at SBMRI.

Phosphotyrosine STAT5 flow cytometric analysis. Aliquots of macrophage and peripheral blood cells were taken to confirm phenotypic identification and phosphotyrosine STAT5 analysis by flow cytometry as previously described.[16,19]

GM-CSF and PGE2 production analysis. After incubation, half of media volume from bone marrow and peritoneal macrophage cultures was collected and frozen at −80°C to measure GM-CSF concentration by Luminex (Upstate Biotech Beadlyte kits, Upstate/Millipore) and enzyme-linked immuosorbent assay (ELISA; BD Biosciences OptiEIA kits, San Diego, CA, USA) as well as PGE2 by ELISA (GE/Amersham, Piscataway, NJ, USA) as previously described.[13,15]

PGS2/COX2 western blot analysis. Peritoneal macrophage cultures were also extracted for protein analysis to detect PGS2/COX2. Cultures of 5×10^6 lavage cells were incubated for 1 hour at 37°C/5% CO_2 to allow for macrophage adhesion. Nonadherent cells were washed off with sterile 1 × PBS and the adherent cells extracted by sonication in SDS lysis buffer (Upstate/Millipore) + protease inhibitors (Roche). Extracts were frozen at −80°C until analysis. Thawed extracts were resuspended with 5 × Leammli sample buffer (Tris–HCL [pH 6.5], 50% glycerol, 1% SDS, 1% 2-mercaptoethanol, 0.1% bromophenol blue, made with reagents from Fisher Scientific, Pittsburgh, PA, USA) and heated to 100°C for 3 minutes. Fifty microliters of each sample was run on 4%–20% acrylamide gels and transferred to Odyssey polyvinylidene floride (PVDF) membranes for western blot analysis using anti-COX2 polyclonal antibodies from Cayman Chemicals (Ann Arbor, MI, USA) and detection using the Li-Cor anti-Rabbit IR700 dye conjugates fluorescence at 700 nm on a Li-Cor Odyssey IR Imaging system (Li-Cor Biosciences, Lincoln, NE, USA).

Sequence analysis of *Csf2* gene promoter and *Ptgs2* enhancer region. Genomic DNA from each strain was prepared from liver of each strain and amplified in PCR using Roche Biosciences Master Mix reagents and primers (3′ CTA AAG CAT GTT TCT TGG CTA; 5′ AAA TAA GGT CCA GCC CAA TG; Integrated DNA Technologies, Coralville, IA, USA) designed to amplify the −3 to −969 bp sequence upstream of the *Csf2* gene.[6,7] The amplified DNA was gel purified using Qiagen gel extraction reagents and phenol/chloroform extracted (Qiagen, Valencia, CA, USA). The amplified fragment was then used as template in a Big Dye PCR amplification reaction (Applied Biosystems, Foster City, CA, USA) and sequenced using an AB capillary sequence analyzer (Applied Biosystems). ChromasLite and ClustalW freeware were used for the sequence analysis and alignment. Overlapping sequence region is depicted in Figure 2. Sequence analysis of the region between *Il10* and *Ptgs2* genes on mouse Chr 1 did not reveal any sequence polymorphisms unique to the NOD mouse or its congenics as compared with C57BL/6 and C57L mice other than the already reported length polymorphisms between these strains detectable by Massachusetts Institute of Technology (MIT) marker analysis.[17,18]

ChIP and ChIP multiplex format analysis. Four to five million cells from bone marrow cultures or ex vivo peritoneal macrophages were fixed in situ with 1% formaldehyde in 1 × PBS (methanol-free, Sigma-Aldrich) for 10 minutes at 37°C prior to lysis with SDS lysis buffer (Upstate/Millipore). The fixed lysates were sonicated to disrupt membranes and shear chromatin to approximately 1,000-bp fragments then frozen until analysis. Once thawed, the samples were divided into aliquots for each run of the analysis. For single-ChIP analyses, aliquots used for IP were precleared with salmon sperm DNA Protein A or G agarose beads (Upstate/Millipore), then incubated overnight at 4°C with antityrosine phosphorylated STAT5 (STAT5Ptyr) antibodies (Upstate/Millipore).

For multiplex format analyses, macrophage extracts were thawed and precleared of nonspecific DNA and Protein G binding proteins by incubation in situ with salmon sperm-Protein G–coated sepharose beads (UpState/Millipore) and bead-free supernatants aliquoted equally over eight PCR microtubes in a strip/capped format (Eppendorf, Westbury, NY, USA). The aliquots were diluted with ChIP dilution buffer (16.7 mM Tris–HCl [pH 8.1], 0.01% SDS, 1.1% Triton X-100, 1.2 mM ethylene diamine tetraacetate (EDTA), 167 mM NaCl; Sigma-Aldrich and Fisher Scientific reagents) to a total volume of 200 µL each. Salmon sperm–Protein G sepharose beads (Upstate/Millipore) were preincubated with 1 µg/30 µL beads suspension in a 96-tube *Multiplex* format using parallel ChIP isolations with one tube of each of the following Upstate/Millipore ChIP–certified antibodies: anti-STAT5Ptyr, anti-RNA polymerase II, antiacetylated histone H3, anti-P300/anti-CBP acetylase, and anti-SMRTe deacetylase. Thirty microliters of the antibody-bead mixes was added to six of the seven tubes of sample, with the final tube being left unprecipitated to act as a total DNA control.

After incubation, the antibody-bound chromatin complexes were precipitated using salmon sperm DNA Protein G agarose beads and washed extensively with a series of increasing stringency buffers (low salt, high salt, LiCl, Tris-EDTA (TE); ChIP reagent kit, Upstate/Millipore). A nonspecific antibody control (mouse IgG, Upstate/Millipore) and a no extract sham IP were run as negative controls in both single and multiplex format ChIP analyses. Total cell and ChIP extract aliquots were dissociated from the beads in 1% SDS, 0.1 M bicarbonate buffer (Fisher Scientific). NaCl was then added to a final concentration of 500 mM and the samples incubated for 4 hours at 65°C to reverse the formaldehyde crosslinks. DNA was purified from these aliquots for PCR and real-time PCR amplification of DNA sequences from *Csf2* promoters, which have been shown to be epigenetic regulatory sites for inducible *Csf2* expression,[6,7] and from the *Ptgs2* enhancer STAT5 binding site.[2]

Real-time PCR was run using Sybr Green Master Mixes (Applied Biosystems or BioRad, Hercules, CA, USA) with the same hot-start protocol designed to remove secondary structure in the DNA template. A cycle profile of 98°C 5 minutes, 94°C 30 sec, 55°C–60°C (dependent on the primer set used) 30 sec, 72°C 30 sec, for 45 cycles, was used.

Real-time amplification quantitation was compared on the basis of the *R*-value calculated as $R = 2^{((\text{Nonspecific Ig ChIP } \Delta Ct)—(\text{anti-STAT5Ptyr ChIP } \Delta Ct))}$.[21] Statistical analyses of data were performed using Prism 5/6 software (GraphPad, San Diego, CA, USA).

Results

Sequence analysis of *Csf2* promoter region defines STAT5 binding site polymorphisms. Sequence analysis of the *Csf2* promoter region was done in all congenic strains and compared in a ClustalW sequence alignment analysis (Figs. 1 and 2). B6.NODC11b and the NOD.LC11e mice share an overlapping NOD genetic region in the *Csf2* promoter that does not extend into the *Csf2* coding region (Fig. 2).

NOD STAT5Ptyr and GM-CSF phenotypes segregate with the NOD *Csf2* promoter. NOD.LC11 and NOD.LC11b mice develop a strong peri-islet insulitis, which remains noninvasive despite having autoreactive T cells present in their T cell population; however, the NOD.LC11e mice developed invasive and destructive insulitis that resulted in overt diabetes.[17] In contrast, pancreatic tissue analyzed from B6.NODC11b and B6.NODC1tb mice shows very little infiltration, mainly limited to periductal areas of the pancreas near islets (data not shown).

Both strains exhibit increased STAT5 phosphorylation (Fig. 3A and C) and GM-CSF expression (Fig. 3B and D), indicating that the overlap region delineates the genetic

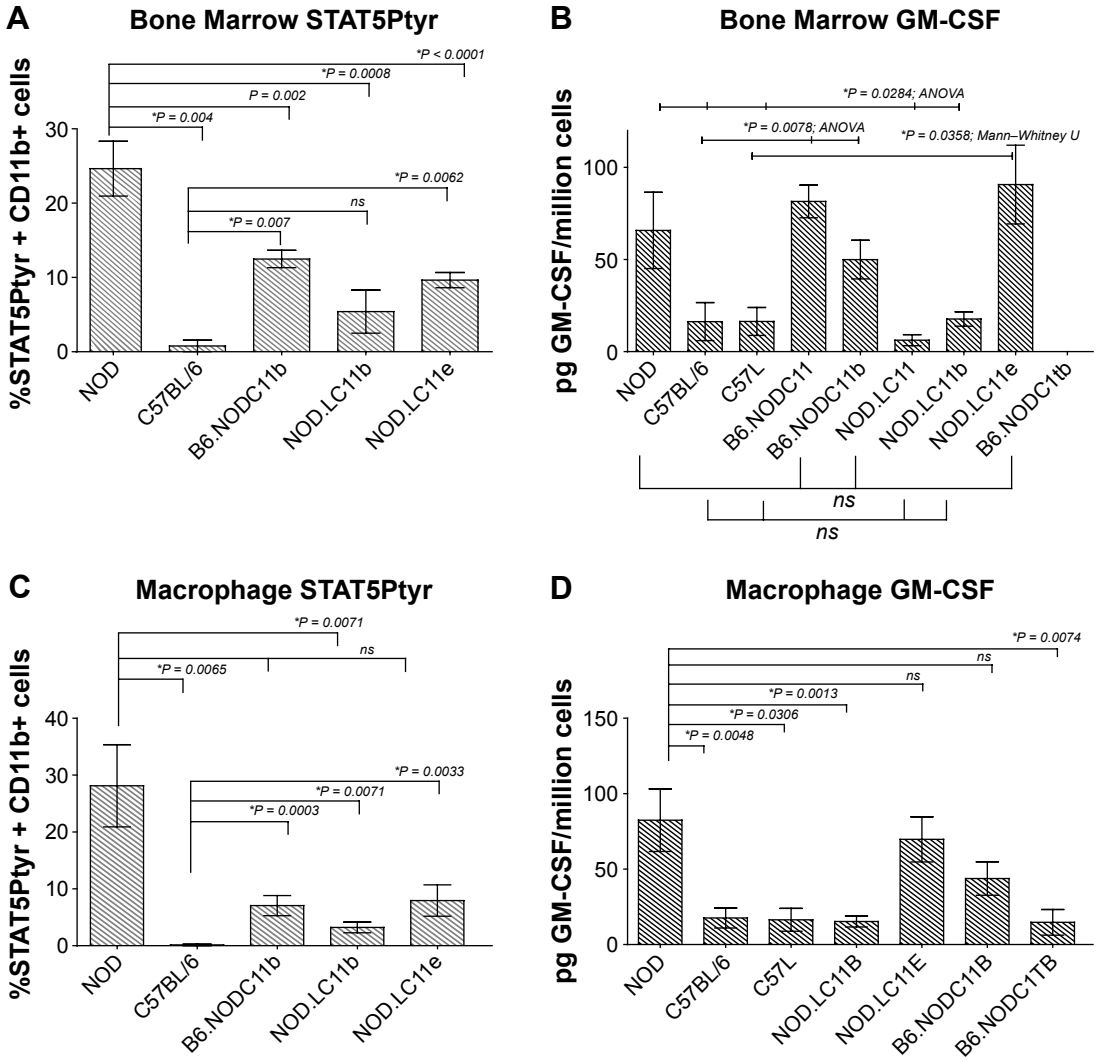

Figure 3. STAT5Ptyr GM-CSF and PGE2 phenotypes for B6.NOD and NOD.L congenic mouse bone marrow cells and peritoneal macrophages. Bone marrow cells (**A** and **C**) and peritoneal macrophages (**B** and **D**) were isolated from female mice of each strain immediately processed for STAT5Ptyr flow cytometry (**A** and **B**) or cultured for 24 hours at 37°C/5% CO_2 without stimulation. Cell-free supernatants from these unstimulated cultures were then analyzed by Luminex or ELISA for GM-CSF (**B** and **D**). Both bone marrow and macrophages from NOD and strains carrying the *Csf2* promoter sequences from the NOD ancestor (NOD, NOD.LC11e, and B6.NODC11b) exhibited elevated levels of STAT5Ptyr and GM-CSF in their CD11b+ myeloid cells compared with nonautoimmune strains or strains that had this sequence from non-NOD ancestors, C57BL/6 or C57L, and NOD.LC11b mice. Means were compared pairwise with NOD and with C57BL/6 using Mann–Whitney *U*-tests or with all strains via one-way analysis of variance. STAT5Ptyr data are representative of multiple runs of the analysis with a minimum of 2 and a maximum of 66 samples per strain tested. GM-CSF Luminex/ELISA data are representative of multiple runs of the analysis with a minimum of 2 and a maximum of 25 samples per strain tested.

locus most likely responsible for the GM-CSF and STAT5 phenotypes seen in the NOD. This shared B6.NODC11b and NOD.LC11e region contains at least one NOD unique potential STAT5 *GAS* binding (TTC**NNN**GAA) and two altered STAT6 *GAS* binding sites (TTC**NNNN**GAA)[22] and includes the regions previously defined as epigenetic regulatory sites.[6,7] Of note, the levels of STAT5Ptyr in Chr11 congenic strains on both NOD and nonautoimmune genetic backgrounds were significantly higher than in nonautoimmune strains but did not reach the levels seen in the NOD (Fig. 3A and C); whereas, the GM-CSF production of these strains were comparable to that seen in NOD myeloid cells (Fig. 3B and D). These data suggest that other NOD genetic components may be influencing the activation and/or persistence of STAT5Ptyr.

STAT5 chromatin binding at the *Csf2* promoter in myeloid cells was also defined by the presence of NOD sequence in this region (Fig. 4). Untreated ex vivo macrophages of NOD mice had enhanced STAT5Ptyr chromatin binding (>56,000-fold above the C57BL/6 control strain) at the site as did macrophages of the B6.NODC11b strain (30-fold higher than the C57BL/6 strain) (Fig. 4A). In contrast, NOD.LC11e congenic mouse macrophages did not have STAT5Ptyr binding at the *Csf2* site. These data indicate that NOD genetic sequence in the promoter of *Csf2* not its coding sequence influence the ability of STAT5Ptyr to bind to this region and potential influence GM-CSF expression and activation of STAT5.

NOD *Csf2* promoter polymorphisms affects STAT5 binding at the *Ptgs2* enhancer. The high GM-CSF production of NOD and T1D human myeloid cells can enhance the

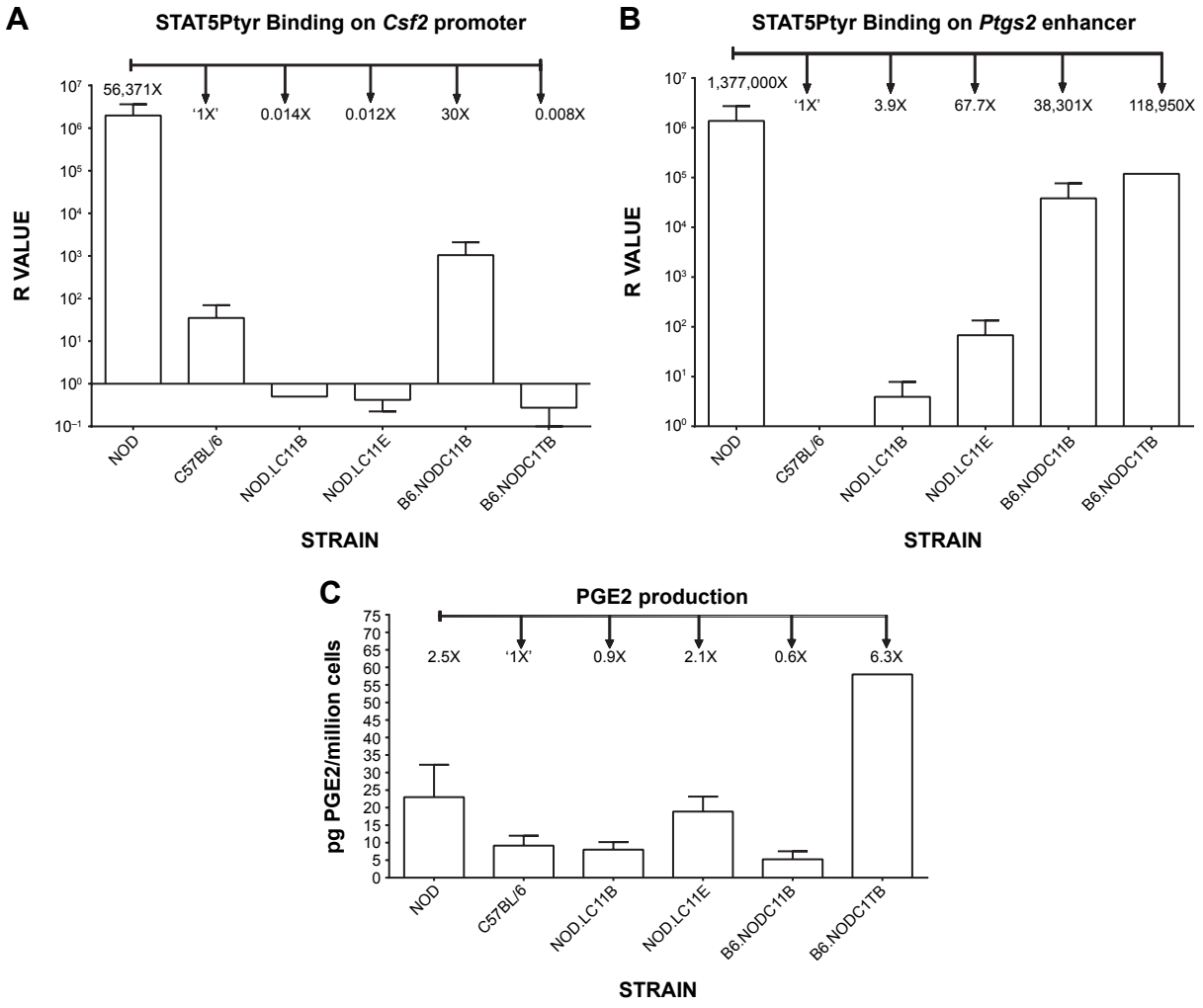

Figure 4. B6.NOD and NOD.L congenic mice STAT5 binding at the *Csf2* promoter and *Ptgs2* enhancer regions. Peritoneal macrophages were isolated from female mice of each strain and cultured for 24 hours at 37°C/5% CO_2 without stimulation. Cultured cells were then fixed and extracted for ChIP analysis using anti-STAT5Ptyr antibodies to isolate STAT5-associated chromatin amplified in real-time PCRs using primers specific for (**A**) the Chr 11 *Csf2* promoter region[6,7,19] and (**B**) the *Il10-Ptgs2* Chr1 region.[2,18] Bars depict mean log *R*-values with standard error of the mean error bars. Data are representative of at least three runs of the analysis. (**C**) Cell-free supernatants were collected for PGE2 analysis by ELISA. Data are representative of at least two runs of the analysis. Bars depict mean with standard error of the mean error bars. Due to unequal variance in the subgroups, no accurate statistical testing was possible. Fold increases for each parameter and each strain as compared to the C57BL/6 nonautoimmune control strain are indicated on the graphs.

PGS2/COX2 production of these cells, even without additional activation stimuli, such as by lipopolysaccharide (endotoxin) (LPS).[13,15] ChIP analysis of macrophage STAT5Ptyr binding at an enhancer site upstream of the *Ptgs2* gene indicated that NOD sequence at the Chr11 *Csf2* promoter affected STAT5Ptyr binding at the Chr1 interval between *Il10-Ptgs2* even in B6.NODC11b mice, which do not have NOD sequence on Chr1 (>38,000-fold higher than seen in the C57BL/6 strain, Fig. 4B). However, mice that had NOD sequence at the Chr 1 *Il10-Ptgs2* region without NOD sequence at the *Csf2* promoter (ie, NOD.LC11b, NOD.LC11e, and B6.NODCt1b) also showed STAT5Ptyr binding above the level seen in C57BL/6J and C57LJ control macrophages (Fig. 4B, data not shown). These findings give evidence that both sites can influence the ability of STAT5Ptyr to bind at the Chr1 interval.

PGE2 production was measured as an indicator of PGS/COX expression. The production of this prostaglandin in unstimulated peritoneal macrophages mirrored the STAT5 binding at the *Ptgs2* enhancer (Fig. 4C). PGE2 production was increased in macrophages of mice that had NOD genetic sequence at the Ptgs2 site on Chr1. Thus, GM-CSF–activated STAT5 binding at the *Csf2* promoter may play a role in proinflammatory dysregulation of the *Ptgs2* gene promoting aberrant expression of PGS2/COX2 in NOD macrophages, other factors besides GM-CSF are influencing PGS2/COX2 expression.

Bicongenic B6.NODC11bxC1tb has STAT5-mediated interaction between Chr 11 *Idd4.3* and Chr 1 *Idd5* with aberrant PGS2/COX2 expression and autoimmune diabetes pathology. To directly test the epigenetic interaction of the *Idd4.3* Chr 11 locus with the Chr 1 locus in the activation of aberrant PGS2/COX2 expression, we cross-bred the recombinant B6.NODC11b strain mice with B6.NODC1tb mice to create a bicongenic strain, B6.NODC11bxC1tb. This strain has two recombination-shortened NOD *Idd* loci (130.8–149.7 Mb,of *Idd5* on Chr 1 and at 53.85 Mb of *Idd4.3* on Chr11) on C57BL/6 genetic background. These bicongenic mice have NOD defined regulatory regions that are dysregulated through cytokine-induced gene activation. Our analyses of these mice confirmed that the STAT5-mediated interaction between these two loci promoted persistent STAT5Ptyr- (Fig. 5A) and STAT5Ptyr-mediated binding epigenetic phenotypes at these loci (Fig. 6), as seen in the NOD ancestor. In addition, the B6.NODC11bxC1tb mice with only these two NOD-derived loci developed an invasive myeloid cell infiltration, hyperglycemia, and apparent immunopathological islet beta cell destruction in approximately 12% to 22% overall (8%–12% [females] and 16%–30% [males]) of the animals by age 30 weeks (Fig. 5C–G).

Unlike their B6.NODC11b congenic progenitors, the GM-CSF production in the B6.NODC11bxC1tb mice was not as high as in the NOD (Fig. 5B). Unstimulated macrophage PGS2/COX2 expression was seen in NOD, bicongenic, and tri-congenic strains, but not in the nondiabetic control strains (Fig. 5H). PGE2 production by B6.NODC11bxC1tb macrophages were higher than that seen in the NOD (Fig. 5I). These data suggest that a specific level of GM-CSF expression and/or other genes (eg, *Irf-1, Il4, Il3*) also regulated by the regional epigenetic control in the Chr 11 *Idd4.3* or in the Chr 1 *Idd5* regions (eg, *Il10*) may be affected by STAT5Ptyr binding to influence *Ptgs2* expression.

In NOD and B6.NODC11bxC1tb macrophages, STAT5Ptyr binding at both the *Csf2* promoter and *Ptgs2* enhancer was found in association with CBP/P300 histone acetylase, acetylated histone H3, and RNA polymerase II at these same sites (Fig. 6). In B6.NODC11bxC1tb macrophage, deacetylase SMRT/NCoR was detected in association with STAT5Ptyr binding at the *Csf2* promoter but not at the *Ptgs2* enhancer. In contrast, C57BL/6 macrophages had markedly lower binding of all but SMRT/NCoR deacetylase at the *Ptgs2* site. Overall binding differences were not statistically significant with the exception of SMRT/NCoR binding being higher in B6.NODC11bxC1tbxC17 cells than in the C57BL/6 cells ($P = 0.0293$, Mann–Whitney *U*-test, 95% confidence level). Both CBP/P300 and SMRT/NCoR binding in the B6.NODC11bxC1tb appeared modestly higher than seen in the C57BL/6 ($P = 0.0519$, Mann–Whitney *U*-test, 90% confidence level).

Congenic addition of *Idd1* to B6.NODC11xC1tb background enhances penetrance but is not required for autoimmune diabetes pathology. The unique MHC of the NOD is not required for the immunopathology seen in the B6.NODC11bxC1tb mice. Congenic breeding addition of the NOD MHC locus (*Idd1* Chr17; B6.NODC11bxC1tbxC17 mice, Fig. 1) did increase the incidence of diabetes to overall 23% to 42% (25 to 53% of males and 22 to 24% of females), as measured by hyperglycemia, invasive immune cell infiltration, and beta cell loss in the pancreas (Figs. 1, 5, and 6). The addition of the *Idd1* locus to the B6.NODC11bxClt1b background did enhance the STAT5Ptyr activation in monocytes (Fig. 5A) but decreased GM-CSF production (Fig. 5B) and STAT5Ptyr binding at the *Csf2* promoter and the *Ptgs2* enhancer compared to B6.C11bxC1tb macrophages (Fig. 6). B6.NODC11bxC1tbXC17 had lower STAT5Ptyr binding at both *Csf2* and *Ptgs2* sites than either NOD or B6.NODC11bxC1tb progenitors, but the presence of CBP/P300, acetylated histone H3, and RNA polymerase II in B6.NODC11bxC1tbXC17 macrophages at both *Csf2* and *Ptgs2* regulatory sites suggest these cells still have the potential for epigenetic and transcriptional activity in these regions. The binding of SMRT/NCoR deacetylase binding at these sites is enhanced in the NOD, bicongenic, and tri-congenic macrophages as well, suggesting that deacetylation regulation is also affected by the genetic changes seen in these diabetic-prone strains.

Discussion

Autoimmune myeloid cell overproduction of GM-CSF induces persistent activation of STAT5Ptyr, with aberrant DNA binding and subcellular localization.[13,19,23] Our previous congenic mouse analyses revealed that the STAT5Ptyr

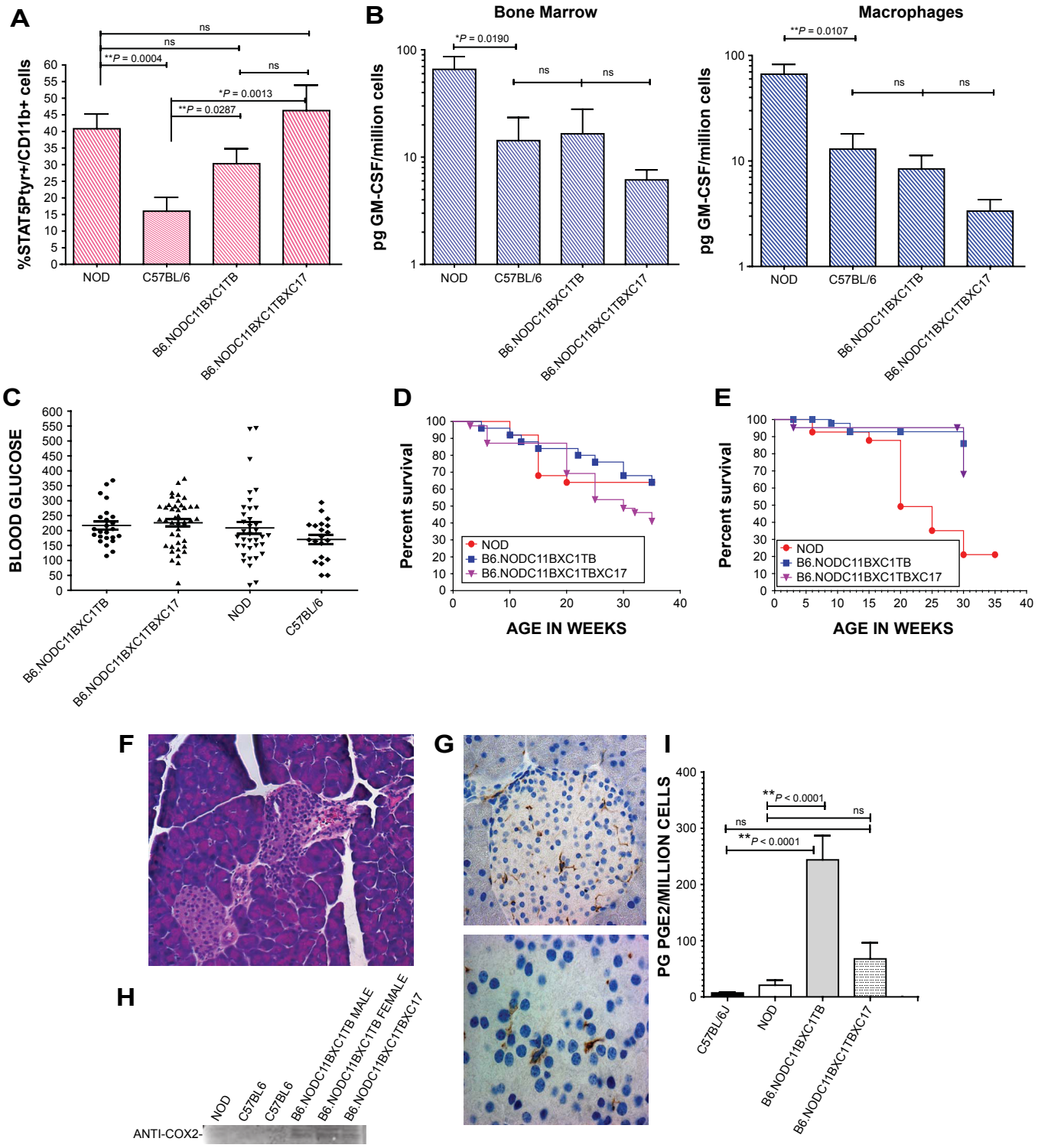

Figure 5. Phenotypic analyses of multicongenic B6.NODC11bxC1tb and B6.NODC11bxC1tbxC17 mice. (**A**) STAT5Ptyr activation in macrophages, (**B**) GM-CSF production by myeloid bone marrow cells (left) and macrophages (right), and (**C**) blood glucose levels of NOD, C56BL/6, and congenic mice. Survival curves of diabetes incidence in NOD, B6.NODC11bxC1tb, and B6.NODC11bxC1tbxC17 mice based on (**D**) blood glucose. (**E**) Invasive beta cell destructive insulitis. (**F**) Invasive insulitis in a B6.NODC11bxC1tb male mouse shown at 20 × magnification. (**G**) Macrophage marker F4/80 immunohistochemical staining in islets of B6.NODC11bxC1tb mice shown at 20 × (upper) and 100 × (lower) magnification. (**H**) Western blot analysis of PGS2/COX2 Expression in 5×10^6 unactivated NOD, C57BL/6, B6.NODC11bxC1tb, and B6.NODC11bxC1tbxC17 mouse peritoneal macrophages. (**I**) ELISA analysis of macrophage PGE2 production of NOD, C57BL/6, and congenic mice. Note that multiple isoforms of PGS2/COX2 appear to be present with different isoforms predominant in the different strains (eg, NOD and C57BL/6 have a longer isoform predominant compared to the congenic strains). STAT5Ptyr, GM-CSF, and PGE2 data are representative of at least three runs of each assay and survival/diabetic phenotype testing are the results from continuous monitoring of 20–30 animals per stain over 6 months in a longitudinal study. Bars (**A**, **B**, and **H**) and horizontal line (**C**) indicate means with standard error of the mean error bars. *P* values for pairwise and one-way analyses of variance are depicted above the data in graphs (**A**, **B**, **C**, and **I**).

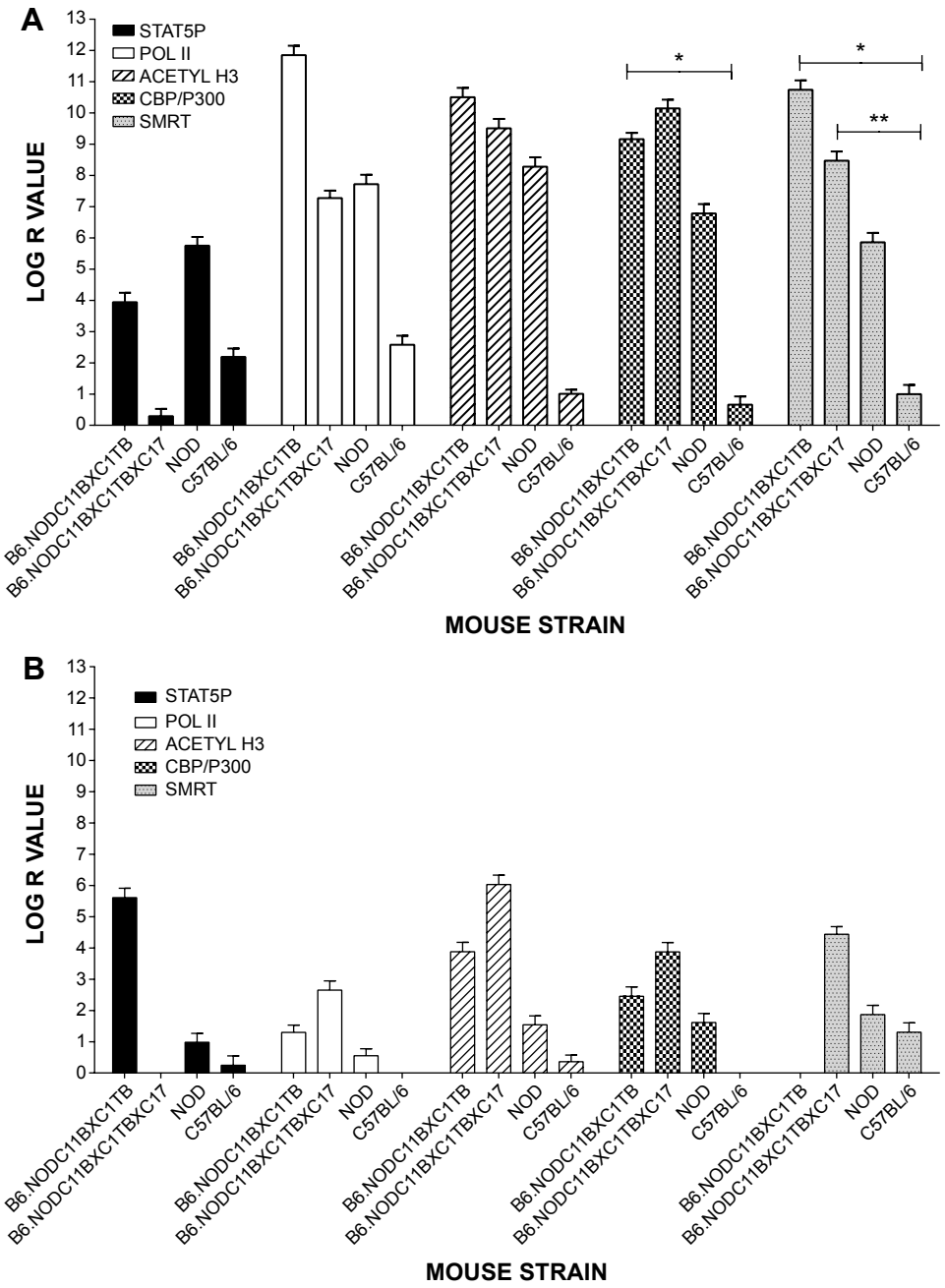

Figure 6. Multicongenic mice multiplex ChIP analysis of STAT5 binding at the *Csf2* promoter and *Ptgs2* enhancer regions. (**A**) Multiplex ChIP analyses for protein association with the Chr11 *Csf2* promoter in NOD, C57BL/6, B6.NODC11bxC1tb, and B6.NODC11bxC1tbxC17 mouse unstimulated peritoneal macrophages cultured for 2 hours at 37°C/5% CO_2. (**B**) Multiplex ChIP analyses done as in (**A**) for epigenetic factor binding/action at *Il10-Ptgs2* Chr1 locus containing enhancer elements for *Ptgs2*. Parallel ChIP analyses in the multiplex were precipitated with antibodies against STAT5Ptyr (STAT5P), RNA polymerase II (POLII), acetylated histone H3 (ACETYL H3), CBP/P300 histone acetylase (CBP/P300), and SMRT/NCoR histone deacetylase (SMRT). Bar pattern key indicates protein associated with the chromatin; bars indicate mean log *R*-value of real-time PCR-specific amplification with standard error of the mean error bars. Mann–Whitney *U*-tests were performed between all pairs of data, indicating that no statistically significant differences were found in any of the data except in CBP/P300 and SMRT bindings indicated: **P* = 0.0519 between B6.NODC11bxC1tb and C57BL/6 CBP/P300 and SMRT binding; ***P* = 0.0293 between B6.NODC11bxC1tbxC17 and C57BL/6 SMRT binding.

and GM-CSF traits seen in the NOD are linked to unique polymorphisms in the *Idd4.3* diabetes susceptibility region of NOD chromosome 11. The sequence within the implicated *Idd4.3* region contains the gene for GM-CSF, *Csf2*, along with several other cytokines that use STAT5Ptyr activation in their signaling.[13,17]

STAT5Ptyr binding in NOD and NOD congenic mouse myeloid cells at both in the *Csf2* promoter and at an enhancer site near *Ptgs2* was enhanced by the presence of a polymorphism at the *Csf2* promoter loci. These data suggest that the polymorphisms in the *Csf2* promoter may be directly involved in all four phenotypes of NOD myeloid cells: GM-CSF

overproduction,[15] prolonged STAT5 activation, STAT5Ptyr dysfunctional chromatin binding,[13,19] and aberrant PGS2/COX2 expression.[13,15,24] Though the same phenotypes are seen in T1D human monocytes, similar polymorphisms are not found in the human analogs of the NOD *Ptgs2* and *Csf2* regions.[14] Further study is needed to determine if strength of bind and/or cooperative binding by other STAT proteins or other proteins also involved in modulating epigenetic modification promote these phenotypes in humans.

As some of our earlier work on GM-CSF induction of STAT5 activation suggested, this study's findings also indicate that continuous GM-CSF overproduction may not be necessary for STAT5Ptyr binding and epigenetic dysregulation of *Ptgs2*, though GM-CSF expression appears to be necessary to initiate STAT5 dysfunction in bone marrow myeloid precursor cells.[13,15,23] The expression of other genes within the Chr 11 *Idd4.3* region (eg, *Il3, Il4, Il5, Irf1*) and/or within Chr 1 *Idd5* (eg, *Il10*) may be affected by STAT5Ptyr binding in these regions to modulate the expression of *Ptgs2* and the role of STAT5Ptyr activation in the different roles of GM-CSF in differentiation and activation still needs to be elucidated.

A major question arising from these findings is how could GM-CSF, PGS2/COX2, and STAT5Ptyr dysfunctions be playing such an important role in diabetes immunopathology as to override the effects of nondiabetic MHC? One possibility is the role of these proteins in myeloid cell differentiation and promotion of chronic inflammation. Myeloid antigen-presenting cell (APC) dysfunction in autoimmunity has been linked to defects in myeloid cell differentiation and diminution of their tolerogenic functions in the presence inflammatory cytokines and prostanoids.[23–25] Myeloid APC differentiation is disrupted in the NOD mouse by defective M-CSF signaling not linked to a lack of either M-CSF or its receptor's expression in these cells, but to dysfunctional intracellular signaling in myeloid cells after binding of M-CSF to its receptor.[25] GM-CSF regulates myeloid cell responsiveness to M-CSF,[1] is essential for inflammatory responsiveness,[2,3] shares signaling pathways with M-CSF,[4] and is highly overexpressed in autoimmune human and mouse myeloid cells.[13–15] The progression of myeloid cell differentiation to mature tolerogenic monocytes, macrophages, and dendritic cells is dependent on temporally and quantitatively regulated GM-CSF stimulation.[1] After maturation, GM-CSF acts as an activation signal in monocytes and macrophages and promotes proinflammatory cytokine and prostanoid production by these cells. In NOD and B6.NODC11bxC1tb bicongenic mice, this regulation appears to be corrupted by the continual presence of activated STAT5Ptyr and its altered binding on epigenetic regulatory sites within the *Csf2* gene promoter.

Aberrant PGS2/COX2 production of PGE2 by autoimmune monocytes and macrophages has been shown to promote chronic inflammation and to interfere with dendritic cell maturation and tolerance induction in mixed DC, macrophage, T cell cultures from NOD mice.[24] High PGS2/COX2 expression has been directly correlated to increased risk in persons carrying high-risk human leukocyte antigen (HLA) alleles and its overproduction of proinflammatory prostanoids such as PGE2 by myeloid cells prohibits CD25 expression and suppressor T cell functions in DQβ 0302/0201 individuals.[26]

STAT5 binding on the *Csf2* promoter Chr11 site also affects GM-CSF stimulation of *Ptgs2* expression, apparently through stimulating STAT5 binding at the *Ptgs2* gene enhancer on Chr1. Since this enhancer sequence lies between the *Il10* gene and the *Ptgs2* gene, it is feasible that GM-CSF regulation of both these genes' expression may be affected by the enhanced STAT5 binding at the site. Our data support its effects on *Ptgs2* expression and recent studies have revealed that IL-2 activation of STAT5 binding at an enhancer site within the *Il10* gene affects IL-10 expression in T cells in diabetic mice[1,27,28] and affects STAT5Ptyr activation specifically in T regulatory cells.[29,30] GM-CSF can stimulate IL-10 expression during resolution of inflammation and may be its influence on the *Il10* gene in myeloid cells may also be via STAT5 binding at this intragene noncoding enhancer region examined in this study. If changes such as length polymorphisms and/or possible insulator sequences are found in the intervening region between the *Il10* and *Ptgs2* genes, these changes may influence the activation of *Ptgs2* gene downstream and the *Il10* gene upstream.

In the presented study, we found that GM-CSF activation of STAT5 binding at epigenetic regulatory sites within the *Csf2* gene promoter altered regulation of its own expression as well as that of *Ptgs2*, the gene for the proinflammatory PGS2/COX2. Thus, aberrant STAT5 binding can affect the expression of two separate loci on separate chromosomes. Bicongenic B6.NODC11bxC1tb mice containing just these two NOD loci, can develop autoimmune diabetes pathology with a low but consistent penetrance. Taken together, these data suggest that B6.NODC11bxC1tb mice define a genetic model for T1D that can promote autoimmune diabetic pathology via an inducible epigenetic regulatory mechanism on a nonautoimmune genetic background.

The findings of this study indicate that epigenetic gene dysregulation may be a potent mechanism by which autoimmune diabetes genetic susceptibility associated with *Idd* loci can aberrantly be activated via induced cytokine signaling. STAT5 dysfunction in autoimmune myeloid cells can facilitate this immunopathological mechanism, as may the yet undiscovered dysfunction of other components of the epigenetic chromatin modification machinery in autoimmune cells.

Acknowledgments

The authors thank UF Pathology, Ramona Bober and her KSC-SLSL vivarium team, and the Charles River SBMRI Animal Care. Martha Campbell-Thompson, DVM/PhD of the UF Pathology Core and John Shelley of the SBMRI Histology Core provided excellent support for our studies. The authors also gratefully acknowledge the generous support of Dr. James Crawford, PhD/MD of this protracted study. Our sincere

gratitude to Dr. Edward Wakeland, PhD of University of Texas Southwestern Medicine Center for expert counsel and Stephanie Dickstein of SBMRI for editorial review of the manuscript.

Author Contributions

Conceived and designed the experiments: SAL. Collection and analysis of the data: EG, NSB, FS, ZH, JC, MM, CW, J-DS, AD-S, JA, AC, TP, CR, MAmick, CH-L, MCS, CW, L-JY, SAL. Wrote the first draft of the manuscript: EG, ZH, NSB, SAL. Contributed to the writing of the manuscript: EG, ZH, NSB, JA, MAtkinson, MSC, MM, SAL. Agree with manuscript results and conclusions: EG, MSB, FS, ZH, JC, MM, LM, ABP, MCS, MAtkinson, CW, AD-S, J-DS, CH-L, L-JY, JA, AC, TP, CR, MAmick, SAL. Jointly developed the structure and arguments for the paper: EG, MCS, MAtkinson, MM, SAL. Made critical revisions and approved final version: MM, MCS, MAtkinson, SAL. All authors reviewed and approved of the final manuscript.

REFERENCES

1. Hashimoto S, Komuro I, Yamada M, Akagawa KS. IL-10 inhibits granulocyte-macrophage colony-stimulating factor-dependent human monocyte survival at the early stage of the culture and inhibits the generation of macrophages. *J Immunol*. 2001;167:3619–3625.
2. Yamaoka K, Otsuka T, Niiro H, et al. Activation of STAT5 by lipopolysaccharide through granulocyte-macrophage colony-stimulating factor production in human monocytes. *J Immunol*. 1998;160:838–845.
3. Hamilton JA. GM-CSF in inflammation and autoimmunity. *Trends Immunol*. 2002;23(8):403–408.
4. Barahmand-Pour F, Meinke A, Kielinger M, Eilers A, Decker T. A role for STAT5 family transcription factors in myeloid differentiation. *Curr Top Microbiol Immunol*. 1996;211:121–128.
5. Piazza F, Vlens J, Lagasse E, Schindler C. Myeloid differentiation of FdCP1 cells is dependent on Stat5 processing. *Blood*. 2000;96(4):1358–1365.
6. Ito K, Barnes PJ, Adcock IM. Glucocortoid receptor recruitment of histone deacetylase 2 inhibits interleukin-1β-induced histone H4 acetylation on lysines 8 and 12. *Mol Cell Biol*. 2000;20(18):6891–6903.
7. Chen X, Wang J, Woltring DS, Gerondakis S, Shannon MF. Histone dynamics on the interleukin-2 gene in response to T-cell activation. *Mol Cell Biol*. 2005; 25(8):3209–3219.
8. Foegh ML. Immune regulation by eicosanoids. *Transplant Proc*. 1988;20(6): 1151–1161.
9. Volk HD, Reinke P, Krausch D, et al. Monocyte deactivation-rationale for a new therapeutic strategy in sepsis. *Intensive Care Med*. 1996;22(suppl 4):S474–S481.
10. Nakajima H, Brindle PK, Handa M, Ihle JN. Functional interaction of STAT5 and nuclear receptor co-repressor SMRT: implications in negative regulation of STAT5-dependent transcription. *EMBO J*. 2001;20(23):6836–6844.
11. Pfitzner E, Jahne R, Wissler M, Stoecklin E, Groner B. p300/CREB-binding protein enhances the prolactin-mediated transcriptional induction through direct interaction with the transactivation domain of Stat5 but does not participate in the glucocorticoid response. *Mol Endocrinol*. 1998;12:1582–1593.
12. Smale ST. The establishment and maintenance of lymphocyte identity through gene silencing. *Nat Immunol*. 2003;4(7):607–615.
13. Litherland SA, Grebe KM, Belkin NS, et al. Nonobese diabetic mouse congenic analysis reveals chromosome 11 locus contributing to diabetes susceptibility macrophage STAT5 dysfunction and GM-CSF overproduction. *J Immunol*. 2005; 175(7):4561–4565.
14. Garrigan E, Belkin NS, Alexander JJ, et al. Persistent STAT5 phosphorylation and epigenetic dysregulation of GM-CSF and PGS2/COX2 expression in type 1 diabetic human monocytes. *PLoS One*. 2013;8(10):e76919.
15. Litherland SA, Xie TX, Grebe KM, Li Y, Moldawer LL, Clare-Salzler MJ. IL10 resistant PGS2 expression in at-risk/type 1 diabetic human monocytes. *J Autoimmun*. 2004;22(3):227–233.
16. Litherland SA, Xie TX, Grebe KM, et al. Signal transduction activator of transcription 5 (STAT5) proteins are dysfunctional in autoimmune monocytes & macrophages. *J Autoimmun*. 2005;24:297–310.
17. McDuffie M. Derivation of diabetes-resistant congenic lines from the nonobese diabetic mouse. *Clin Immunol*. 2000;96(2):119–130.
18. Yui MA, Muralidharan K, Moreno-Altamirano B, Perrin G, Chestnut K, Wakeland EK. Production of congenic mouse strains carrying NOD-derived diabetogenic genetic intervals: an approach for the genetic dissection of complex traits. *Mamm Genome*. 1996;7(5):331–334.
19. Seydel F, Garrigan E, Stutevoss B, et al. GM-CSF induces STAT5 binding at epigenetic regulatory sites within the Csf2 promoter of nonobese diabetic (NOD) mouse myeloid cells. *J Autoimmun*. 2008;31(4):377–384.
20. Wakeland E, Morel L, Achey K, Yui M, Longmate J. Speed congenics: a classic technique in the fast lane (relatively speaking). *Immunol Today*. 1997;18(10): 472–477.
21. Nelson JD, Denisenko O, Sova P, Bomsztyk K. Fast chromatin immunoprecipitation assay. *Nucleic Acids Res*. 2006;34(1):e2–e7.
22. Ehret GB, Reichenbach P, Schindler U, et al. DNA binding specificity of different STAT proteins. *J Biol Chem*. 2001;276(9):6675–6688.
23. Rumore-Maton B, Elf J, Belkin NS, et al. M-CSF and GM-CSF regulation of STAT5 activation and DNA binding in myeloid cell differentiation is disrupted in nonobese diabetic mice. *Clin Dev Immunol*. 2008;2008(76795):1–8.
24. Clare-Salzler M. The immunopathogenic roles of antigen presenting cells in the NOD mouse. In: Leiter EH, Atkinson MA, eds. *NOD Mice and Related Strains: Research Applications in Diabetes, AIDS, Cancer, and Other Diseases*. Austin, TX: Landes Bioscience Publishers; 1998:101–120.
25. Serreze DV, Gaskins HR, Leiter EH. Defects in the differentiation and function of antigen presenting cells in the NOD/Lt Mice. *J Immunol*. 1993;150:2534–2543.
26. Litherland SA, Xie TX, Hutson A, et al. Aberrant monocyte prostaglandin synthase 2 (PGS2) expression defines an antigen presenting cell defect and is a novel cellular marker for insulin dependent diabetes mellitus (IDDM). *J Clin Invest*. 1999;104:515–523.
27. Tsuji-Takayama K, Suzuki M, Yamamoto M, et al. The production of IL-10 by human regulatory T cells is enhanced by IL-2 through a STAT5-responsive intronic enhancer in the IL-10 locus. *J Immunol*. 2008;181:3897–3905.
28. Dendrou CA, Wicker LS. The IL-2/CD25 pathway determines susceptibility to T1D in humans and NOD mice. *J Clin Immunol*. 2008;28(6):685–696.
29. Murawski MR, Litherland SA, Clare-Salzler MJ, Davoodi-Semiromi A. Upregulation of Foxp3 expression in mouse and human Treg is IL-2/STAT5 dependent: implications for the NOD STAT5B mutation in diabetes. *Ann N Y Acad Sci*. 2006;1079:198–204.
30. Davoodi-Semiromi A, McDuffie M, Litherland SA, Clare-Salzler MJ. Truncated pSTAT5B is associated with the *Idd4* locus in NOD mice. *Biochem Biophys Res Commun*. 2007;356(3):655–661.